

# Myasthenic nicotinic receptor mutant interpreted in terms of the allosteric model

## *Application du modèle allostérique à l'interprétation d'un mutant myasthénique du récepteur nicotinique musculaire*

STUART J. EDELSTEIN,<sup>1,2</sup> OLIVIER SCHAAD,<sup>1</sup> JEAN-PIERRE CHANGEUX<sup>2\*</sup>

<sup>1</sup> Département de biochimie, université de Genève, CH-1211 Genève 4, Switzerland;

<sup>2</sup> Ura D1284 Neurobiologie moléculaire du CNRS, Institut Pasteur, 25, rue du D'-Roux, 75734 Paris cedex 15, France

### RÉSUMÉ

Un modèle allostérique du type Monod-Wyman-Changeux est étendu aux récepteurs nicotini-ques du muscle humain exprimés dans des cellules HEK. Les propriétés fonctionnelles du récep-teur normal, ainsi que celles du mutant myasthénique  $\epsilon$ T264P, sont examinées de manière quantitative. Le modèle se fonde sur la transition concertée entre l'état basal B (canal fermé) et l'état actif A (canal ouvert). L'équilibre  $B \rightleftharpoons A$  est déterminé en absence d'acétylcholine par la constante allostérique,  $L_0$ , égale au rapport  $[B_0]/[A_0]$ . Lorsque la valeur de  $L_0$  est égale à  $9 \times 10^8$ , le modèle offre une excellente représentation des données enregistrées avec les récepteurs normaux par la méthode du « patch-clamp » ; la distribution des temps d'ouverture du canal est unimodale avec un maximum à 0,7 ms. Le modèle rend compte de la distribution trimodale publiée par Ohno et al. (1995) pour les temps d'ouverture du canal avec le mutant  $\epsilon$ T264P sur la base d'une valeur de  $L_0$  égale à 100. Les trois maxima, à 0,15, 3,8 et 60 ms, sont interprétés comme corres-pondant respectivement aux récepteurs sans, ou avec une, ou deux molécules d'acétylcholine liées. L'application du modèle allostérique à l'interprétation des propriétés physiologiques d'autres mutants myasthéniques est examinée.

**Mots clés :** modèle allostérique, récepteur nicotinique d'acétylcholine, mutant myasthénique, temps d'ouverture de canaux uniques

### ABSTRACT

*An extended Monod-Wyman-Changeux allosteric-type model is applied to human muscle nicotinic acetylcholine receptors expressed in HEK cells, for both the normal form and the high-affinity human myasthenic mutant,  $\epsilon$ T264P. The model is based on a concerted transition between the basal (resting) B state and the active (open-channel) A state, with the equilibrium in the absence of ligand determined by the allosteric constant,  $L_0 = [B_0]/[A_0]$ . For wild-type receptors the model with  $L_0 = 9 \times 10^8$  provides a satisfactory representation of published patch-clamp recordings that yields a distribution of open-channel dwell times with a single peak at 0.7 ms. For the  $\epsilon$ T264P mutant, the model with  $L_0 = 100$  accounts for the trimodal distribution reported for open-channel dwell times, with peaks at 0.15, 3.8 and 60 ms that correspond to non-, mono- and bi-liganded receptors, respectively. Possible applications of the allosteric model to other myasthenic mutants are considered.*

**Key words:** allosteric model, nicotinic acetylcholine receptor, myasthenic channel mutant, single-channel open times

---

Note présentée par Jean-Pierre Changeux

Note remise le 1<sup>er</sup> octobre 1997, acceptée après révision le 27 octobre 1997

---

\*Correspondence and reprints

## VERSION ABRÉGÉE

**Introduction**

Le récepteur nicotinique de l'acétylcholine du muscle est une protéine membranaire composée de cinq sous-unités [ $2\alpha:1\beta:1\delta:1\varepsilon$ ]. La lumière du canal est bordée par les résidus du domaine transmembranaire M2 de chaque sous-unité. Les deux sites de liaison de l'acétylcholine se trouvent aux interfaces des sous-unités  $\alpha/\delta$  et  $\alpha/\varepsilon$ . La fixation de l'acétylcholine stabilise transitoirement l'état A (canal ouvert), puis le récepteur retourne à l'état basal B ou évolue vers des états I ou D (états désensibilisés). Selon le modèle allostérique, ces états s'interconvertissent librement, y compris en absence de ligand, entraînant de ce fait des ouvertures spontanées du canal. De telles ouvertures spontanées ont été parfois observées avec les récepteurs nicotiniques musculaires. Cependant, les enregistrements de canaux uniques ont été le plus souvent interprétés sur la base d'un modèle séquentiel limitant les ouvertures du canal aux récepteurs ligandés. Avec les récepteurs normaux, la rareté des ouvertures spontanées est telle que la distinction entre les prédictions du modèle allostérique et celles du modèle séquentiel n'est pas possible. En revanche, les propriétés du récepteur provenant d'individus atteints d'un syndrome myasthénique congénital consécutif à la mutation  $\varepsilon$ T264P sont telles que la distinction entre les deux modèles devient possible.

**Méthodes**

Le modèle allostérique sous sa forme étendue au cas du récepteur nicotinique comporte au moins quatre états qui sont, respectivement : B (de base, canal fermé mais activable), A (actif, canal ouvert), et deux états désensibilisés (réfractaire et canal fermé), I et D, où l'acétylcholine se lie plus fortement sur D que sur I. Avec une brève application d'acétylcholine, la désensibilisation est négligeable, et les états B et A suffisent pour modéliser les données concernant les récepteurs normaux ainsi que ceux portant la mutation  $\varepsilon$ T264P. Les valeurs des constantes de vitesse de liaison de chaque molécule de ligand, ainsi que celles de l'interconversion entre états allostériques, ont été ajustées aux données publiées avec les récepteurs normaux et avec le mutant  $\varepsilon$ T264P. Des simulations stochastiques d'ouverture du canal ont été obtenues par transformation de ces constantes en probabilités. Les descriptions globales des récepteurs normaux et mutés ont été calculées en termes de distribution d'ouvertures en fonction de la durée de chaque échantillonnage.

**Résultats et discussion****Récepteurs normaux**

Des simulations de canaux uniques ont d'abord été produites avec le modèle allostérique, et comparées aux données publiées avec les récepteurs nicotiniques normaux du muscle humain exprimés dans des cellules HEK. Les prédictions du modèle, obtenues avec une valeur de la constante allostérique  $L_0 = 9 \times 10^8$ , concordent avec les données enregistrées avec

une concentration d'acétylcholine de 0,3 mM. Ces données sont caractérisées par une probabilité d'ouverture  $p_o = 10^{-4}$ , et par une distribution des temps d'ouverture ayant un maximum de 0,7 ms. Dans le cas des récepteurs normaux, à cette concentration d'acétylcholine, les prédictions du modèle allostérique et du modèle séquentiel sont très semblables, du fait du faible taux d'ouvertures spontanées ( $\sim 1$  ouverture/15 s) prédit par le modèle allostérique.

**Récepteurs de myasthéniques avec la mutation  $\varepsilon$ T264P**

Des simulations de canaux uniques ont été obtenues avec le modèle allostérique, et comparées aux données publiées concernant des récepteurs de myasthéniques portant la mutation  $\varepsilon$ T264P et exprimés dans des cellules HEK. Avec  $L_0 = 100$ , ce qui correspond à une probabilité d'ouverture de  $p_o = 0,22$ , le modèle représente de façon satisfaisante les données obtenues avec une concentration d'acétylcholine de 0,3  $\mu$ M, y compris la distribution trimodale des temps d'ouverture. Les trois maxima qui caractérisent la distribution des temps d'ouverture (à 0,15, 3,8 et 60 ms) sont attribués, selon le modèle allostérique, à des molécules de récepteur ayant respectivement lié zéro, une ou deux molécules d'acétylcholine. Un modèle séquentiel, pour lequel les ouvertures coïncident obligatoirement avec les récepteurs ligandés, ne permet pas de rendre compte de ces données.

**Autres récepteurs de myasthéniques**

Treize mutants myasthéniques ont été identifiés à ce jour : les positions de cinq de ces mutations sont exactement homologues de celles déjà introduites et caractérisées avec les récepteurs neuronaux homopentamériques  $\alpha 7$ . Par conséquent, les divers phénotypes des mutants déjà décrits avec les récepteurs  $\alpha 7$  peuvent fournir une base d'interprétation des phénotypes des mutants myasthéniques. Trois classes de phénotypes ont été proposées :  $\gamma$ , L et K.

Le phénotype du mutant  $\alpha 7$  L247T se manifeste par une haute affinité pour l'acétylcholine, un nouvel état de conductance, la conversion d'antagonistes compétitifs en agonistes et un taux important d'ouvertures spontanées. Ces propriétés peuvent être expliquées par un état désensibilisé pour lequel la mutation a rendu le canal ouvert. Un tel changement dans la conductance d'un état est désigné par « phénotype  $\gamma$  ». D'autres mutants du récepteur  $\alpha 7$  de haute affinité, tels que V251T, peuvent être expliqués par une diminution de la constante allostérique,  $L_0$ , et entrent dans la catégorie de « phénotype L ». Un changement uniquement de l'affinité d'un état pour le ligand est désigné par « phénotype K ».

Parmi les treize mutations myasthéniques identifiées, pour onze d'entre elles le syndrome pathologique résulte d'une augmentation d'activité, tandis que pour les deux autres,  $\varepsilon$ P121L et  $\varepsilon$ R311W, les symptômes correspondent à une réduction d'activité. Cependant, seulement quatre des mutants myasthéniques ont été caractérisés en termes de constantes de vitesse :  $\varepsilon$ P121L,  $\alpha 1$  G153S,  $\alpha 1$  N271K et

$\alpha 1$  V249F. Dans ces quatre cas, les propriétés physiologiques ont été interprétées sur la base d'une modification de l'affinité intrinsèque pour l'acétylcholine, ce qui correspond au phénotype K. Deux de ces mutations,  $\epsilon$ P121L et  $\alpha 1$  G153S, sont situées dans le domaine N-terminal, où se trouvent les résidus contribuant aux sites de liaison de l'acétylcholine. Pour cette raison, un phénotype K est plausible, mais une modification de l'équilibre allostérique reste possible. En effet, un phénotype L a été observé avec le mutant  $\alpha 7$  G152K à la position qui correspond à celle du mutant  $\alpha 1$  G153S. La mutation  $\alpha 1$  N271K dans le domaine M1 et la mutation

$\alpha 1$  V249F dans le domaine M2 se trouvent à une distance importante des sites de liaison de l'acétylcholine, et des interprétations basées sur un phénotype L sont plausibles.

En conclusion, l'analyse du mutant T264P sur la base du modèle allostérique rend compte des données obtenues par enregistrements de canaux uniques avec une valeur de la constante allostérique ( $L_0$ ) nettement diminuée par rapport à la valeur attribuée aux récepteurs normaux. Des modifications de la valeur de  $L_0$  pouvaient aussi être considérées avec les autres mutants myasthéniques, afin d'éclaircir les mécanismes responsables des phénotypes pathologiques observés.

## Introduction

The muscle nicotinic acetylcholine receptor (nAChR) is a heteropentameric (2 $\alpha$ :1 $\beta$ :1 $\delta$ :1 $\epsilon$ ) integral membrane protein, with an axial ion channel bordered by the M2 transmembrane segment and the two acetylcholine (ACh) binding sites at the interfaces between each  $\alpha$  subunit and its neighboring  $\delta$  or  $\epsilon$  subunit [1–3]. Interactions with ACh elicit two distinct chemical reactions: the stabilization of the receptor in an open conformation (A) initiating a transient ion flux that terminates by a return to the basal (resting) state (B) or the transition to a high affinity desensitized state (I or D). Understanding the molecular basis for the coupling between ligand binding and channel opening represents a major challenge for structural biology that ultimately must await determination of the three-dimensional structure at atomic resolution. Nevertheless, establishing plausible functional models will play an essential role in providing the mechanistic framework within which to interpret structural information.

According to the allosteric-type model, receptors occur with a set of discrete, spontaneously interconverting conformational states [4]; concerted transitions to the open-channel conformation are favored by the higher affinity of agonist for the A state, but can in principle occur even in the absence of ligand [5, 6]. Although such spontaneous openings have been observed under certain conditions for muscle-type receptors [7–9], most mechanistic analyses have been based on sequential-type models [10–14] along the lines of the induced-fit mechanism [15]. The sequential models assume that the ion channel opens only upon binding of two ligand molecules (or possibly with one molecule in the case of brief openings) and thus do not account for the occurrence of spontaneous openings. However, a consensus has not yet emerged concerning which model most closely describes the physical basis of receptor action. Uncertainties exist as well concerning the degree to which differences in the affinities of the two binding sites are responsible for characteristic properties of the nAChR. While differences of up to 700-fold have been reported [16–21], in other studies the results have been interpreted with two equivalent sites [11–14]. Significantly different mechanistic models may in appearance provide satisfactory representations of a

particular data set. For example, recent data concerning the properties of human muscle nAChR expressed in HEK cells have been interpreted in terms of a rather wide range of ligand binding affinities [14,19–21], varying from a 350-fold difference for the affinity of the two sites in the B state [19] to identical affinities for the two sites [14].

Additional insights into the functional mechanism of nAChR have been provided by mutant receptors. Over the last few years, an increasing number of mutations in the human population responsible for congenital myasthenic syndromes have been identified [14,19–26]. A particularly interesting example is the myasthenic mutant  $\epsilon$ T264P that lies in the channel-forming M2 domain. When expressed in HEK cells, receptors with this mutation exhibit spontaneous channel opening and a trimodal distribution of open times [19]. Since no mechanistic interpretations were provided for this mutant, we have examined these data and as reported here the allosteric model provides a straightforward explanation, principally on the basis of a large decrease in the value of  $L_0$ , the equilibrium constant governing the transition between the B and A states.

## Methods

The allosteric model for the nAChR includes four conformational states that differ in their affinity for agonists (and antagonists) and the rates at which they interconvert [5]: the closed but activatable B (basal) state; the open-channel A (active) state; and the I and D states (desensitized) which are refractory to activation. For the applications presented here, only activation is considered, since data concerning the desensitized states are not available for the  $\epsilon$ T264P mutant receptors. The relevant reactions for the allosteric model involving the B and A states are presented in *figure 1*. Values of the appropriate rate constants for wild-type and mutant receptors (see *table 1*) were incorporated into the overall rate matrix and converted to transition probabilities per unit time as described previously [5]. Stochastic simulations are presented for wild-type and mutant receptors as a train of events extending over 0.1 s (*figure 2*) or as a complete description of the sto-

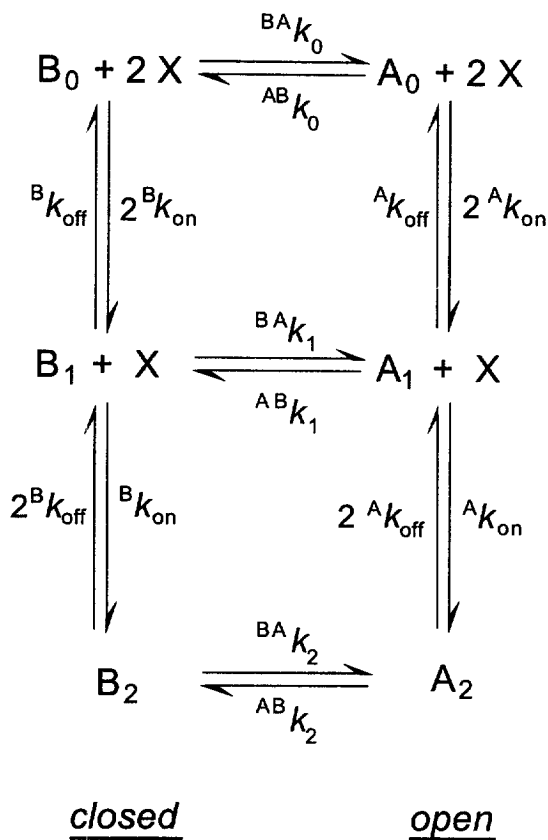


**Figure 1.** Conformational states and ligand binding reactions for nAChR with two agonist binding sites as formulated by the allosteric model.

Interconversion reactions for receptors in the B and A states at varying degrees of ligation are indicated by the subscript 0, 1 or 2. Equilibrium constants are defined from the appropriate kinetic constants (i.e.,  ${}^B K = {}^B k_{\text{off}} / {}^B k_{\text{on}}$ ,  ${}^A K = {}^A k_{\text{off}} / {}^A k_{\text{on}}$ , and  $L_0 = {}^{AB} k_0 / {}^{BA} k_0$ ). According to linear free energy relations [5], the interconversion rates vary with the ratio of affinities of the B and A states (where  ${}^{BA} c = {}^A K / {}^B K$ ), as modulated by the transition state position parameter,  ${}^{BA} p$ , such that  $\log ({}^{AB} k_i / {}^{AB} k_{i,1}) = {}^{BA} p \log ({}^{BA} c)$  and  $\log ({}^{BA} k_{i,1} / {}^{BA} k_i) = (1 - {}^{BA} p) \log ({}^{BA} c)$ . In relation to the standard model [11], the opening and closing rates ( $\alpha_2$  and  $\beta_2$ ) are defined by  $\alpha_2 = {}^{AB} k_2$  and  $\beta_2 = {}^{BA} k_2$ . Therefore, from measured values of  ${}^{AB} k_2$  and  ${}^{BA} k_2$ , the values of the other interconversion rate constants are fixed by  ${}^{BA} c$  and  ${}^{BA} p$ .

chastic behavior using the probability density function [27, 28] of the dwell times (figure 3).

## Results and discussion

### Wild-type receptors

Simulations of the stochastic properties of single channel openings based on the allosteric model were generated for wild-type nAChR for 0.3  $\mu\text{M}$  ACh. Typical progressions through the various molecular species are described in figure 2a, with those events corresponding to channel opening indicated. The corresponding dwell-time probabilities are presented in figure 3a. At the low concentration of ACh used for the simulation, ionic events for wild-

**Table I.** Parameters for wild-type and mutant nAChR.

	Wild type	$\epsilon\text{T264P}$
<i>Ligand binding</i>		
${}^B k_{\text{on}}$ ( $\times 10^8 \text{ M}^{-1} \text{ s}^{-1}$ )	1.0	1.0
${}^A k_{\text{on}}$ ( $\times 10^8 \text{ M}^{-1} \text{ s}^{-1}$ )	1.0	1.0
<i>Ligand dissociation</i>		
${}^B k_{\text{off}}$ ( $\text{s}^{-1}$ )	$1.65 \times 10^4$	$7.56 \times 10^3$
${}^A k_{\text{off}}$ ( $\text{s}^{-1}$ )	0.1	4.4
<i>Interconversion steps</i>		
${}^{BA} k_0$ ( $\text{s}^{-1}$ )	$2.06 \times 10^{-4}$	65.8
${}^{BA} k_1$ ( $\text{s}^{-1}$ )	3.08	$3.94 \times 10^3$
${}^{BA} k_2$ ( $\text{s}^{-1}$ )	$4.60 \times 10^4$	$2.4 \times 10^5$
${}^{AB} k_0$ ( $\text{s}^{-1}$ )	$1.86 \times 10^5$	$6.58 \times 10^3$
${}^{AB} k_1$ ( $\text{s}^{-1}$ )	$1.68 \times 10^4$	$2.29 \times 10^2$
${}^{AB} k_2$ ( $\text{s}^{-1}$ )	$1.52 \times 10^3$	8.0

For wild-type nAChR the parameters were based on measurements of human muscle receptors expressed in 293 HEK cells [14, 21]. The values for  ${}^{AB} k_2$  and  ${}^{BA} k_2$  were set by the published values of  $\alpha_2$  and  $\beta_2$ , respectively, with the other interconversion rates calculated using linear free-energy relations on the basis of the value of the transition state parameter,  ${}^{BA} p = 0.2$  [5]. Values for the A state were obtained by principles of microscopic reversibility. The ratio  ${}^{AB} k_0 / {}^{BA} k_0$  yields a value of the primary constant for the allosteric transition,  $L_0 = 9 \times 10^8$  for the wild-type nAChR. For the  $\epsilon\text{T264P}$  mutant,  ${}^{AB} k_0$  and  ${}^{AB} k_2$  were calculated using the  $\tau_0$  and  $\tau_2$  values reported for 0.3  $\mu\text{M}$  ACh [22]. For  ${}^{AB} k_1$ , the value derived from  $\tau_1$  (see legend to figure 3) was corrected to 229  $\text{s}^{-1}$ , since according to linear free energy relations it should be intermediate between  ${}^{AB} k_0$  and  ${}^{AB} k_2$  on a logarithmic scale [5]. The analysis was based on  $\tau_0$  and  $\tau_2$  values, since it was assumed that these values would be subject to fewer errors of estimation than  $\tau_1$ , for which the data overlap with contributions of both of the other time constants. This estimation of parameter values for  $\epsilon\text{T264P}$  results in  ${}^{BA} p = 0.45$ ,  $L_0 = 100$ , and the rates listed for  ${}^{BA} k_0$ ,  ${}^{BA} k_1$ , and  ${}^{BA} k_2$  deduced according to linkage principles and free energy relations. While the change in the value of  $L_0$  dominated the properties of the  $\epsilon\text{T264P}$  mutant, the fit to the data was improved by additional changes in  ${}^B k_{\text{off}}$  and  ${}^A k_{\text{off}}$ .

type receptors are predicted to be infrequent, corresponding to a probability of channel opening of  $P_0 = 10^{-4}$ . The simulation in figure 2a includes one event for each open-channel species,  $A_0$ ,  $A_1$  and  $A_2$ , and their overall probabilities presented in figure 3a display a single peak with an average open-channel dwell time of 0.7 ms. The predictions of the allosteric model, based on a value of the allosteric constant  $L_0 = 9 \times 10^8$ , are in excellent agreement with the data points (o) obtained from the kinetic constants reported [21] to describe an extensive data set for human muscle receptors expressed in HEK cells. Concerning the range of ligand binding affinities reported [14, 19–21], it is clear that more than one set of rate constants can provide an apparent description of the same data set of single channel events. Therefore, in order to establish the true degree of equivalence of the two binding sites, direct ligand binding measurements would be required [29].

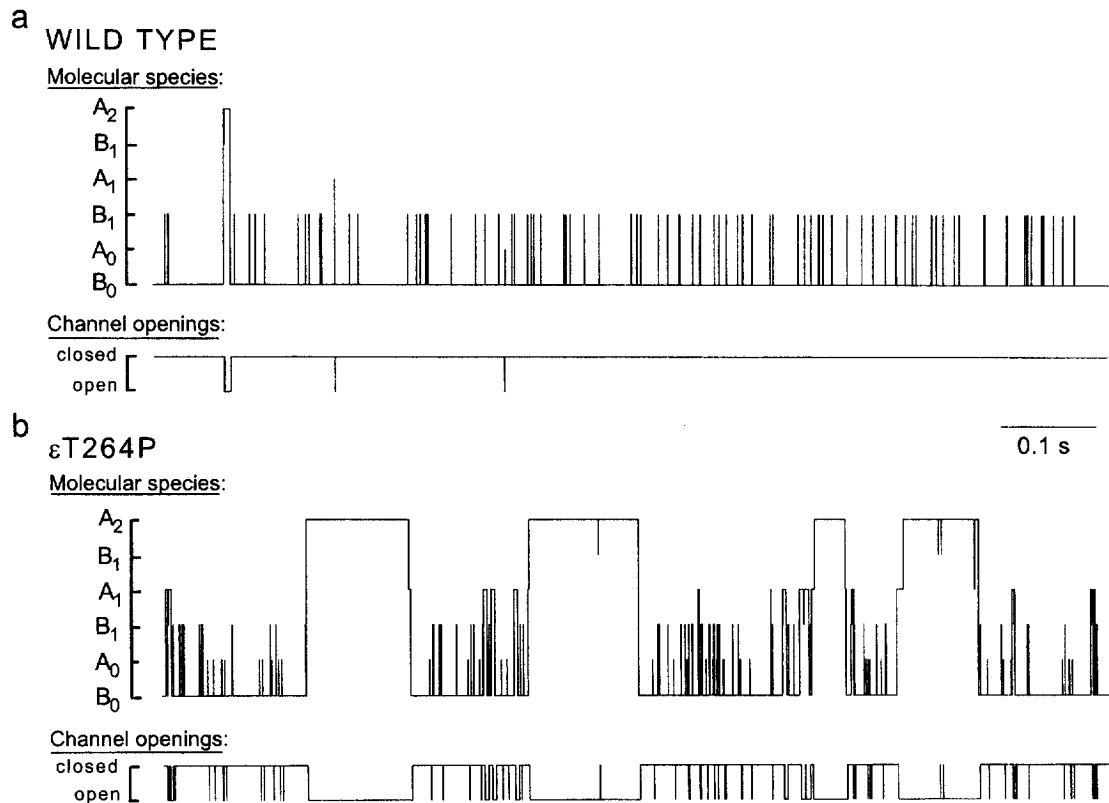


**Figure 2. Stochastic simulations for the nAChR.**

**a. Wild-type. b. Mutant εT264P.**

The simulations were conducted for  $0.3 \mu\text{M}$  ACh using the parameter values listed in table I. Each simulation shows the progression in time through the various molecular species. Each passage through the A state is registered as a channel opening in the trace aligned below the molecular species.

The simulations demonstrate that for wild-type receptors the allosteric model can represent patch-clamp data in as satisfactory a manner as the sequential-type models (figure 3a). Whether critical experiments can be designed to distinguish between the models remains to be ascertained. The principal difference concerns channel opening in the absence of ligand. While such events are predicted only by the allosteric model, for wild-type receptors they are expected to be rare ( $\sim 1/15$  s) and rapid ( $\sim 5 \mu\text{s}$ ), and may therefore escape detection. More favorable conditions for examining the possibility of spontaneous channel opening are provided by mutant receptors, including pleiotropic site-directed channel mutants first observed for neuronal  $\alpha 7$  nAChR [30–32] and subsequently with muscle nAChR [24, 33, 34], as well as related receptors for other neurotransmitters [35, 36]. Certain naturally occurring myasthenic mutants may provide similar advantages and for this reason the properties of the high-affinity mutant  $\epsilon\text{T264P}$  have been examined in detail.

#### $\epsilon\text{T264P}$ mutant receptors

Simulations for the myasthenic mutant  $\epsilon\text{T264P}$  based on the published data for receptors expressed in HEK cells

[22] are presented in figure 2b. Although a complete kinetic analysis was not included in the initial description of the  $\epsilon\text{T264P}$  receptors, the amplitudes and average time constants for the trimodal distribution of channel opening events were presented for  $0.3 \mu\text{M}$  ACh [22]. Simulations corresponding to the properties described for this ACh concentration were obtained using a markedly lower value of the isomerization constant,  $L_0 = 100$ , compared to the wild-type value of  $L_0 = 9 \times 10^8$  (table I). The effect of lowering  $L_0$  is distributed throughout the interconversion rate constants, both raising the  $B \rightarrow A$  rates and lowering the  $A \rightarrow B$  rates (table II). The result of such an ‘L phenotype’ [37] is a facilitation of the  $B \rightarrow A$  transition and thus a substantial increase in the sensitivity to agonist. In the absence of ACh, the probability of spontaneous channel opening becomes measurable (frequency  $\sim 2/\text{s}$  and duration  $\sim 0.1$  ms) and at  $0.3 \mu\text{M}$  ACh the probability of opening is  $P_o = 0.22$ , which contrasts with the wild-type value of  $P_o = 10^{-4}$  (figure 3b). Furthermore, the assumption of a diminished value of  $L_0$  leads to the prediction of three distinct peaks in the dwell-time profiles of opening events with average open-channel dwell times of 0.15, 3.8 and 60 ms. At this stage, with the available data,

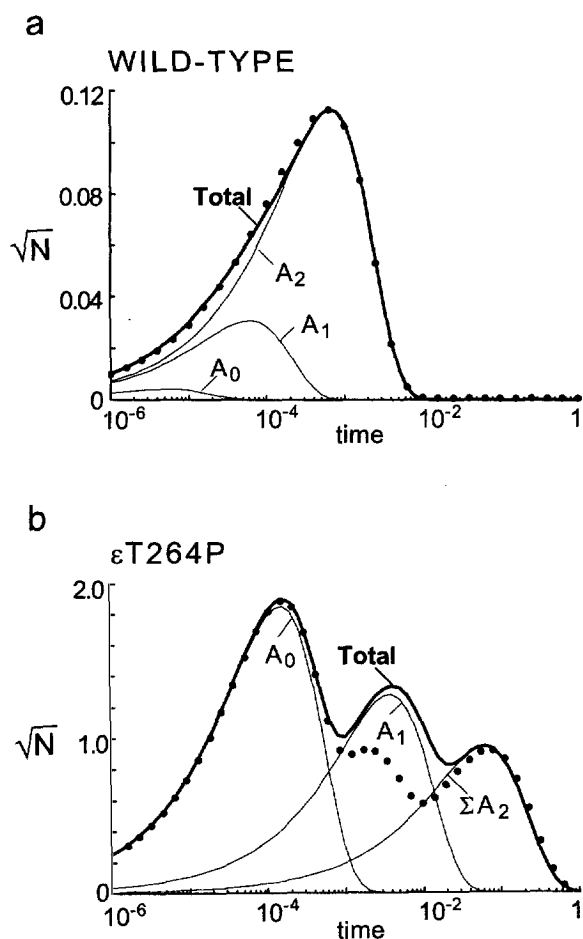


**Figure 3.** Open-channel dwell times for stochastic simulations of single channel events.

**a. Wild-type.**

**b. Mutant  $\epsilon$ T264P.**

The dwell-time profiles probability density function [27, 28], with the square root of the number of events versus time on a logarithmic scale, present the predicted distribution of all species (thick line) and the contributions of the individual components (thin lines) for simulations as described in figure 2 for an ACh concentration of  $0.3 \mu\text{M}$ . At this concentration,  $P_0 = 10^{-4}$  for the wild-type nAChR and  $P_0 = 0.22$  for the mutant  $\epsilon$ T264P, where:  $P_0 = 1/(1 + ((L_0 l(X)^B K + 1)^2)/(X^B K + 1)^2))$ , with the ligand concentration indicated by  $X$  and the equilibrium constants as defined in the legend to figure 1. For wild-type receptors in **a**, the individual points (o) are obtained from the kinetic rate constants presented in the legend to figure 8b of the article by Milone et al. [21] to represent activation over a wide range of ACh concentrations. For  $\epsilon$ T264P receptors in **b**, the individual points (o) are presented for the sum of the three phases of the experimentally observed open dwell times corresponding to the published values [22] for  $0.3 \mu\text{M}$  ACh of  $\tau_0 = 150 \mu\text{s}$ ,  $a_0 = 0.67$ ;  $\tau_1 = 1.8 \text{ ms}$ ,  $a_1 = 0.16$ ; and  $\tau_2 = 69.5 \text{ ms}$ ,  $a_2 = 0.17$ , where  $\tau_i$  and  $a_i$  are the mean open time and relative amplitude, respectively, for each component. The contributions to the pdf for  $\epsilon$ T264P of  $A_2$  channel opening involve passage to  $B_2$ , as well as passage to  $A_1$ , and the sum of both processes is indicated by  $\Sigma A_2$  (in **b**). The simulations corresponding to ten bins for each integer interval of  $\log t$ , with peak heights based on the number of events occurring in a total time  $t$  of 1 s.

alternative explanations for the three peaks based on receptors with different subunit stoichiometry, e.g.,  $\alpha_2\beta\gamma\epsilon$ ,

$\alpha_2\beta\gamma_2$ , and  $\alpha_2\beta\epsilon_2$ , have not been ruled out, yet the atypical structures with two  $\gamma$  or two  $\epsilon$  subunits have only been observed when the missing subunit had been omitted from the expression system [8]. Further studies in which the proportions of the different subunits expressed are varied should in principle clarify this issue. In addition, different patterns of dependence on agonist concentration would be expected for populations of fixed sites compared with a homogeneous population of interacting sites.

The trimodal pattern predicted by the allosteric model is compared to the three peaks reported for recombinant  $\epsilon$ T264P receptors [22] and represented in figure 3b by the individual points (o) calculated by summing the three experimentally observed components. As expected from the kinetic derivation of the allosteric model [5], the greater the number of ligands bound, the longer the average dwell time for channel opening. The initial fitting in figure 3b gives a reasonably satisfactory agreement between theory and experiment, considering the difficulties in extracting the parameters from the three overlapping experimental curves and the relatively limited quantity of data reported [22]. On the basis of this analysis, the three peaks for the mutant receptors may be readily interpreted in terms of the allosteric model as reflecting non-, mono- and bi-liganded receptors (figure 3b). The sequential-type models, which do not include open states for non-liganded receptors [11, 14, 21] cannot satisfactorily represent such data. The sequential schemes contrast with the basic postulate of the allosteric model according to which the conformational equilibrium is established prior to ligand binding (figure 1).

### Other myasthenic mutant receptors

The physiological properties of the 13 myasthenic mutants identified to date are summarized in table II. For five of these cases, the position of the point mutation corresponds to a site previously mutated in the homopentameric neuronal receptor  $\alpha 7$  and characterized on the basis of the functional properties of the mutant form expressed in oocytes. Hence, the phenotypes observed for the  $\alpha 7$  site-directed mutants can provide an initial basis for the interpretation of the myasthenic mutants and the relevant  $\alpha 7$  mutants, along with their proposed phenotypic interpretation, are also presented in table II. Three classes of phenotypes have been distinguished:  $\gamma$ , L and K [37]. The pleiotropic phenotype observed for the  $\alpha 7$  L247T mutant in the M2 channel domain includes a high affinity for ligand, a new conductance state, conversion of competitive antagonists into agonists, and spontaneous opening [30–32]. This mutant can be understood in terms of a high-affinity desensitized state that has been rendered conducting (a ‘ $\gamma$  phenotype’). Other high affinity mutants in the channel such as V251T [38] can be satisfactorily represented by a decrease in the equilibrium constant,  $L_0$ , governing the allosteric transition between the B and A states that renders the A state more favorable (an ‘L phe-

**Table II. Myasthenic mutations and site-directed mutations at corresponding positions in chick  $\alpha 7$ .**

Domain	Muscle			Neuronal $\alpha 7$		
	Myasthenic	Properties	Proposed interpretation	Site-directed	Properties	Proposed interpretation
N-terminal	$\epsilon$ P121 L	weak response [20]	K/L phenotype, but see [20]	$\alpha 7$ P120	–	n.d.
	$\alpha 1$ G153S	prolonged openings [19]	K/L phenotype, but see [19]	$\alpha 7$ G152K	low $EC_{50}$ and $IC_{50}$ [40]	L phenotype
	$\alpha 1$ V156M	prolonged openings [25]	K/L phenotype	$\alpha 7$ L155I	normal $IC_{50}$ [40]	WT phenotype
M1	$\alpha 1$ N217K	prolonged openings [14]	L phenotype, but see [14]	$\alpha 7$ N 213	–	n.d.
	$\epsilon$ P245L	prolonged openings [26]	L phenotype	$\alpha 7$ L 231	–	n.d.
M2	$\alpha 1$ V249 F	spontaneous openings [21]	L phenotype, but see [21]	$\alpha 7$ V245	–	n.d.
	$\beta$ L262M	prolonged openings [24]	L phenotype	$\alpha 7$ L247T	spontaneous openings [30, 32]	$\gamma$ phenotype
	$\alpha 1$ T254I	prolonged openings [25]	L phenotype	$\alpha 7$ T250	–	n.d.
	$\epsilon$ T264P	spontaneous openings [22]	L phenotype	$\alpha 7$ T250	–	n.d.
	$\beta$ V266M	spontaneous openings [23]	L phenotype	$\alpha 7$ V251T	low $EC_{50}$ [38]	L phenotype
	$\epsilon$ L269F	spontaneous openings [23]	L phenotype	$\alpha 7$ L255	–	n.d.
M2-M3 loop	$\alpha 1$ S269I	prolonged openings [25]	L phenotype	$\alpha 7$ D265N	high $EC_{50}$ [39]	L phenotype
M3	$\epsilon$ R311W	shortened openings [26]	L phenotype	$\alpha 7$ 297H	–	n.d.

notype'). An L phenotype can also produce lower apparent affinity by an increase in  $L_0$ , as proposed in *table II* for the  $\alpha 7$  mutant D265N [39]. Mutations producing a direct effect on ligand binding affinity may also occur (a 'K phenotype'), particularly at the ligand binding site [37], although for mutations in this region a modification of L may also be produced, as proposed for  $\alpha 7$  G152K [40].

For each of the myasthenic mutants it is of interest to evaluate whether its properties can be attributed predominantly to one of these phenotypes. However, in contrast to  $\epsilon$ T264P analyzed in detail as reported here, data for the other 12 mutants are not available in a form suitable for conducting a similar analysis and only four of the mutants have been characterized in terms of individual rate constants:  $\epsilon$ P121L,  $\alpha 1$  G153S,  $\alpha 1$  N217K and  $\alpha 1$  V249F [14,19–21]. Nevertheless, an initial attempt to establish the phenotype can be made on the basis of the available reports and the resulting 'proposed interpretation' is presented for each of the myasthenic mutants in *table II*. Overall, pathological syndromes can be caused by either

'gain' or 'loss' of function. For the 13 examples presented in *table II*, 11 of the mutations identified involve gain of function, with loss of function occurring only for  $\epsilon$ P121L and  $\epsilon$ R311W. The myasthenic mutants are distributed throughout the receptor structure and include examples in the N-terminal domain that encompasses the ligand binding sites, as well as other examples in three of the transmembrane domains and the M2–M3 loop. Each group of mutations is considered below.

For myasthenic mutations in the M2 domain the most simple hypothesis is to invoke interpretations in terms of the L phenotype (*table II*), by analogy with the  $\alpha 7$  mutations. Evidence for such a phenotype is provided for several of the M2 mutants by the occurrence of spontaneous openings, generally characteristic of a receptor with a marked decrease in the value of  $L_0$  [37]. For most of these mutants insufficient data were provided to permit a complete kinetic analysis, but for the  $\alpha 1$  V249F mutation, the novel properties were interpreted in terms of an increase in the affinity of one of the binding sites from the micro-

molar to the nanomolar range [21]. However, future studies should also explore whether a satisfactory interpretation can also be provided by an L phenotype. Indeed, a change solely in the affinity of ligand binding at one site by over three orders of magnitude would be difficult to reconcile with the fact that the position of the mutation is far from the ligand binding sites and occurs on both  $\alpha 1$  subunits. Moreover, this mutation occurs at the position adjacent to the site homologous to the  $\alpha 7$  mutation T244Q [38], which was interpreted by us on the basis of an L phenotype [37]. The explanation involving one high-affinity site for  $\alpha 1$  V249F is based mainly on the bursting properties at low ligand concentrations (10 nM ACh) attributed to multiple  $B_2 \leftrightarrow A_2$  interconversions. However, desensitization is also markedly enhanced in this mutant, resulting in no detectable channel activity at ACh concentrations in the  $\mu M$  range. Therefore, an alternative explanation for the bursting could be provided by transitions to the desensitized state, along the lines observed for wild-type receptors at higher concentrations [41]. Such a mechanism could be readily described by a multi-state allosteric model that includes the kinetic events leading to desensitization [5]. An allosteric-type mechanism based on an L phenotype is also supported by the fact that the spontaneous open channels ( $\sim 1/s$ ) were observed with this mutant [21].

For the myasthenic mutations in transmembrane regions M1 and M3, as well as in the M2–M3 loop, we also propose interpretations based on an L phenotype (table II). However, the properties observed for the mutation  $\alpha 1$  N217K were interpreted by the authors as an increase in affinity ( $\sim 10$ -fold) for both (in this case equivalent) binding sites [14]. In this case as well, additional studies will be required to determine whether an L phenotype can also satisfactorily represent the data. For the myasthenic mutations in the N-terminal domain, properties involving K and/or L phenotypes may be expected.

**Acknowledgements:** The research described here was supported by the Swiss National Science Foundation, the Association française contre les myopathies, the Collège de France, the Centre national de la recherche scientifique, the Direction des Recherches Etudes et Techniques, EEC Biotech and Biomed, and the Council for Tobacco Research.

## REFERENCES

1. Unwin N. 1993. Neurotransmitter action: opening of the ligand-gated ion channels. *Neuron* 10, 31-41
2. Galzi J.-L., Changeux J.-P. 1994. Neurotransmitter-gated ion channels as unconventional allosteric proteins. *Curr. Opin. Struct. Biol.* 4, 554-565
3. Karlin A., Akabas M.H. 1995. Toward a structural basis for the function of nicotinic acetylcholine receptors. *Neuron* 15, 1231-1244
4. Monod J., Wyman J., Changeux J.-P. 1965. On the nature of allosteric transitions: A plausible model. *J. Mol. Biol.* 12, 88-118
5. Edelstein S.J., Schaad O., Henry E., Bertrand D., Changeux J.-P. 1996. A kinetic mechanism for nicotinic acetylcholine receptors based on multiple allosteric transitions. *Biol. Cybern.* 75, 361-380
6. Edelstein S.J., Changeux J.-P. 1996. Allosteric proteins after thirty years: the binding and state functions of the neuronal (7) nicotinic acetylcholine receptor. *Experientia* 52, 1083-1090
7. Jackson M.B. 1984. Spontaneous openings of the acetylcholine receptor channel. *Proc. Natl. Acad. Sci. USA* 81, 3901-3904
8. Jackson M.B., Imoto K., Mishina M., Konno T., Numa S., Sakmann B. 1990. Spontaneous and agonist-induced openings of an acetylcholine receptor channel composed of bovine  $\alpha$ ,  $\beta$ - and  $\delta$ -subunits. *Pflügers Arch. Eur. J. Physiol.* 417, 129-135
9. Auerbach A., Sigurdson W., Chen J., Akk G. 1996. Voltage dependence of mouse acetylcholine receptor gating: different charge movements in di-, mono-, and unliganded receptors. *J. Physiol.* 494, 155-179
10. Del Castillo J., Katz B. 1957. Interaction at endplate receptors between different choline derivatives. *J. Physiol.* 146, 369-381
11. Colquhoun D., Sakmann B. 1985. Fast events in single-channel currents activated by acetylcholine and its analogues at the frog muscle end-plate. *J. Physiol.* 369, 501-557

For the mutant  $\epsilon P121L$  its 'loss of function' was interpreted by the authors mainly by a lower affinity ( $\sim 50$ -fold) at one of the binding sites [20]. The mutant  $\alpha 1$  G153S leads to a 'gain of function' attributed by the authors to an increase in the affinity ( $\sim 50$ -fold) at one of the binding sites [19], but alternative explanations may be developed involving contributions from an L phenotype, as suggested for the  $\alpha 7$  mutation in the region of the binding site G152K (table II) that alters the apparent affinity for ligand mainly through changes in the equilibria governing the allosteric transitions [40]. Hence, the phenotypes of mutations in the N-terminal domain may include at least a significant contribution from changes in the equilibrium between conformational states in addition to direct changes in the binding site. Such a mixed phenotype is designated 'K/L' in table II.

In conclusion, the unusual channel opening properties reported for the high affinity  $\epsilon T264P$  mutant of the human muscle nAChR provide critical insights into the differences between the allosteric- and sequential-type models. The allosteric-type model predicts significant channel opening for non-liganded, mono-liganded and bi-liganded receptors. However, for wild-type receptors the bi-liganded form dominates even at low ligand concentrations, and opening events in the absence of ligand may be too rare and too rapid to be reliably detected. In contrast, for the mutant  $\epsilon T264P$ , the published high affinity properties are readily interpreted by the allosteric model with a  $B \leftrightarrow A$  equilibrium that lies less strongly in favor of the B state in the absence of ligand compared to wild-type receptors (L phenotype). In this case, the three distinct open-channel dwell times observed can be interpreted in terms of receptors with zero, one or two ligand molecules bound, respectively. Similar principles may be applicable to other myasthenic mutants whose phenotypes have been interpreted with a sequential model that limits channel opening to liganded receptors.

12. Lingle C.J., Maconochie D., Steinbach J.H. 1992. Activation of skeletal muscle nicotinic acetylcholine receptors. *J. Membrane Biol.* 126, 195-217
13. Edmonds B., Gibb A.J., Colquhoun D. 1995. Mechanisms of activation of muscle nicotinic acetylcholine receptors and the time course of endplate currents. *Annu. Rev. Physiol.* 57, 469-493
14. Wang H.-L., Auerbach A., Bren N., Ohno K., Engel A.G., Sine S.M. 1997. Mutation in the M1 domain of the acetylcholine receptor alpha subunit decreases the rate of agonist dissociation. *J. Gen. Physiol.* 109, 757-766
15. Koshland D.E., Némethy G., Filmer D. 1966. Comparison of experimental binding data and theoretical models in proteins containing subunits. *Biochemistry* 5, 365-385
16. Jackson M.B. 1988. Dependence of acetylcholine receptor channel kinetics on agonist concentration in cultured mouse muscle fibers. *J. Physiol.* 397, 555-583
17. Sine S.M., Claudio T., Sigworth F.J. 1990. Activation of *Torpedo* acetylcholine receptors expressed in mouse fibroblasts: single channel current kinetics reveal distinct agonist binding affinities. *J. Gen. Physiol.* 96, 395-437
18. Zhang Y., Chen J., Auerbach A. 1995. Activation of recombinant mouse acetylcholine receptors by acetylcholine, carbamylcholine and tetramethylammonium. *J. Physiol.* 486, 189-206
19. Sine S.M., Ohno K., Bouzat C., Auerbach A., Milone M., Pruitt J.N., Engel A.G. 1995. Mutation of the acetylcholine receptor alpha subunit causes a slow-channel myasthenic syndrome by enhancing agonist binding affinity. *Neuron* 15, 229-239
20. Ohno K., Wang H.-L., Milone M., Bren N., Brengman J.M., Nakano S., Quiram P., Pruitt J.N., Sine S.M., Engel A.G. 1996. Congenital myasthenic syndrome caused by decreased agonist binding affinity due to a mutation in the acetylcholine epsilon subunit. *Neuron* 17, 157-170
21. Milone M., Wang H.-L., Ohno K., Fukudome T., Pruitt J.N., Bren N., Sine S.M., Engel A.G. 1997. Slow-channel myasthenic syndrome caused by enhanced activation, desensitization, and agonist binding affinity attributable to mutation in the M2 domain of the acetylcholine receptor alpha subunit. *J. Neurosci.* 17, 5651-5665
22. Ohno K., Hutchison D.O., Milone M., Brengman J.M., Bouzat C., Sine S.M., Engel A.G. 1995. Congenital myasthenic syndrome caused by prolonged acetylcholine receptor channel openings due to a mutation in the M2 domain of the epsilon subunit. *Proc. Natl. Acad. Sci. USA* 92, 758-762
23. Engel A.G., Ohno K., Milone M., Wang H.-L., Nakano S., Bouzat C., Pruitt J.N., Hutchison D.O., Brengman J.M., Bren N., Sieb J.P., Sine S.M. 1996. New mutations in acetylcholine receptor subunit genes reveal heterogeneity in the slow-channel congenital myasthenic syndrome. *Hum. Mol. Gen.* 5, 1217-1227
24. Gomez C.M., Maselli R., Gammack B.S., Lasalde J., Tamamizu S., Cornblath D.R., Lehar M., McNamee M., Kuncel R.W. 1996. A beta-subunit mutations in the acetylcholine receptor channel gate causes severe slow-channel syndrome. *Ann. Neurol.* 39, 712-723
25. Croxen R., Newland C., Beeson D., Oosterhuis H., Chauplanaz G., Vincent A., Newsom-Davis J. 1997. Mutations in different functional domains of the human muscle acetylcholine receptor alpha subunit in patients with the slow-channel congenital myasthenic syndrome. *Hum. Mol. Gen.* 6, 767-774
26. Ohno K., Quiram P., Milone M., Wang H.-L., Harper M.C., Pruitt J.N., Brengman J.M., Pao L., Fischbeck K.H., Crawford T.O., Sine S.M., Engel A.G. 1997. Congenital myasthenic syndromes due to heteroallelic nonsense/missense mutations in the acetylcholine receptor epsilon subunit gene: identification and functional characterization of six new mutations. *Hum. Mol. Gen.* 6, 753-767
27. Sigworth F.J., Sine S.M. 1987. Data transformations for improved display and fitting of single-channel dwell time histograms. *Biophys. J.* 52, 1047-1054
28. Colquhoun D., Hawkes A.G. 1995. The principles of the stochastic interpretation of ion-channel mechanisms. In: *Single-Channel Recording* (Sakmann, B., Neher, E. eds.), Second Edition, Plenum Press, New York, 397-482
29. Edelstein S.J., Schaad O., Changeux J.-P. 1997. Single bindings versus single channel recordings: a new approach to ionotropic receptors. *Biochemistry* 36, 13755-13760
30. Revah F., Bertrand D., Galzi J.-L., Devillers-Thiéry A., Mulle C., Hussy N., Bertrand S., Ballivet M., Changeux J.-P. 1991. Mutations in the channel domain alter desensitization of a neuronal nicotinic receptor. *Nature* 353, 846-849
31. Bertrand D., Devillers-Thiéry A., Revah F., Galzi J.-L., Hussy N., Mulle C., Bertrand S., Ballivet M., Changeux J.-P. 1992. Unconventional pharmacology of a neural nicotinic receptor mutated in the channel domain. *Proc. Natl. Acad. Sci. USA* 89, 1261-1265
32. Bertrand S., Devillers-Thiéry A., Palma E., Buisson B., Edelstein S.J., Corringer P.-J., Changeux J.-P., Bertrand D. 1997. Paradoxical allosteric effects of competitive inhibitors on neuronal alpha7 nicotinic receptor mutants. *Neuroreport* 8, 3591-3596
33. Labarca C., Nowak M.W., Zhang H., Tang L., Desphande P., Lester H.A. 1995. Channel gating governed symmetrically by conserved leucine residues in the M2 domain of nicotinic receptors. *Nature* 376, 514-516
34. Filatov G.N., White M.M. 1995. The role of conserved leucines in the M2 domain of the acetylcholine receptor in channel gating. *Mol. Pharmacol.* 48, 379-384
35. Yakel J.L., Lagrutta A., Adelman J.P., North R.A. 1993. Single amino acid substitution affects desensitization of the 5-hydroxytryptamine type 3 receptor expressed in *Xenopus* oocytes. *Proc. Natl. Acad. Sci. USA* 90, 5030-5033
36. Chang Y., Wang R., Barot S., Weiss D.S. 1996. Stoichiometry of a recombinant GABA<sub>A</sub> receptor. *J. Neurosci.* 16, 5415-5424
37. Galzi J.-L., Edelstein S.J., Changeux J.-P. 1996. The multiple phenotypes of allosteric receptor mutants. *Proc. Natl. Acad. Sci. USA* 93, 1853-1858
38. Devillers-Thiéry A., Galzi J.-L., Bertrand S., Changeux J.-P., Bertrand D. 1992. Stratified organization of the nicotinic acetylcholine receptor channel. *Neuroreport* 3, 1001-1004
39. Campos-Caro A., Sala S., Ballesta J.J., Vicente-Aguilló F., Criado M., Sala F. 1996. A single residue in the M2-M3 loop is a major determinant of coupling between binding and gating in neuronal nicotinic receptors. *Proc. Natl. Acad. Sci. USA* 93, 6118-6123
40. Corringer P.-J., Bertrand S., Bohler S., Edelstein S.J., Changeux J.-P., Bertrand D. 1997. Identification of critical elements modulating desensitization of neuronal nicotinic receptors. *J. Neurosci.* (in press)
41. Sakmann B., Patlak J., Neher E. 1980. Single acetylcholine-activated channels show burst-kinetics in presence of desensitizing concentrations of agonist. *Nature* 286, 71-73